Frontiers of Information Technology & Electronic Engineering
www.jzus.zju.edu.cn; engineering.cae.cn; www.springerlink.com
ISSN 2095-9184 (print); ISSN 2095-9230 (online)
E-mail: jzus@zju.edu.cn

Chaotic dynamics of a fractional order glucose-insulin regulatory system*

Karthikeyan RAJAGOPAL[‡1,2], Atiyeh BAYANI[3], Sajad JAFARI[3,4],
Anitha KARTHIKEYAN[1], Iqtadar HUSSAIN[5]

[1]*Center for Nonlinear Dynamics, Defence University, Bishoftu 1041, Ethiopia*
[2]*Institute of Energy, Mekelle University, Mekelle 231, Ethiopia*
[3]*Department of Biomedical Engineering, Amirkabir University of Technology, Tehran 159163-4311, Iran*
[4]*Nonlinear Systems and Applications, Faculty of Electrical and Electronics Engineering, Ton Duc Thang University, Ho Chi Minh City 700010, Vietnam*
[5]*Department of Mathematics, Statistics and Physics, Qatar University, Doha 2713, Qatar*
E-mail: rkarthiekeyan@gmail.com; atiyeh.bayani@yahoo.com; sajad.jafari@tdtu.edu.vn;
mrs.anithakarthikeyan@gmail.com; iqtadarqau@gmail.com

Received Feb. 24, 2019; Revision accepted Apr. 14, 2019; Crosschecked Oct. 18, 2019; Published online Dec. 21, 2019

Abstract: The fractional order model of a glucose-insulin regulatory system is derived and presented. It has been extensively proved in the literature that fractional order analysis of complex systems can reveal interesting and unexplored features of the system. In our investigations we have revealed that the glucose-insulin regulatory system shows multistability and antimonotonicity in its fractional order form. To show the effectiveness of fractional order analysis, all numerical investigations like stability of the equilibrium points, Lyapunov exponents, and bifurcation plots are derived. Various biological disorders caused by an unregulated glucose-insulin system are studied in detail. This may help better understand the regulatory system.

Key words: Diabetes mellitus; Chaos; Bifurcation; Multistability; Antimonotonicity
https://doi.org/10.1631/FITEE.1900104 **CLC number:** O415.5

1 Introduction

Diabetes is a common disorder, in which the blood sugar (glucose) level is abnormally high and the body cannot produce enough insulin to use it (Kumar and Sreedevi, 2017). Many mathematical models have been proposed to demonstrate the interaction between insulin and glucose and the dynamics of the diabetes disease in the body (Ackerman et al., 1964; Bajaj et al., 1987; Liszka-Hackzell, 1999; Holt, 2003; Chuedoung et al., 2009). The first attempt to proposing this model goes back to the 1960s when researchers suggested a two-dimensional (2D) differential equation (Ackerman et al., 1964). Considering the effect of β-cells (Bajaj et al., 1987), this model has been improved to nonlinear three-dimensional (3D) equations with different properties which can demonstrate the complex behavior of the body. A new model considers a predator-prey based model, which has shown chaotic behavior (Shabestari et al., 2018). As the arrhythmia in the glucose-insulin regulatory system can cause different types of disorders (type-1 diabetes, type-2 diabetes, hypoglycemia, and hyperinsulinemia), in this study, we propose a model considering different parameters, leading to different types of these diseases.

‡ Corresponding author
* Project supported by the Institute of Research and Development, Defence University, Ethiopia (No. DU/IRD/002)
ORCID: Karthikeyan RAJAGOPAL, http://orcid.org/0000-0003-2993-7182

Proposing mathematical models for biological phenomena can help scientists better understand and even control diseases. Many biological systems are in the category of nonlinear dynamical systems (Baghdadi et al., 2015; Hadaeghi et al., 2016; Aram et al., 2017; Bao H et al., 2018; Ginoux et al., 2019). Chaos, different types of bifurcations (such as the period doubling route to chaos), multistability, and anti-monotonicity are several properties which have been observed in biological systems (Schiff et al., 1994; Preissl et al., 1996; Korn and Faure, 2003), also in diabetes (Ginoux et al., 2018). Nonlinear analyses (like embedding space, correlation dimension, Lyapunov exponents, singular value decomposition, and phase portraits) claim chaotic behavior in experimental glucose and insulin time-series (Hansen, 1923; Lang et al., 1979; Pfeiffer et al., 1993; Kroll, 1999). Also, 48-h immunoreactive insulin measurements from ambulatory-fed subjects indicated chaotic behavior in plasma insulin and glucose patterns (Molnar et al., 1972). Regarding research in which chaotic systems with complex behavior have been analyzed and controlled (Pham et al., 2012; Buscarino et al., 2018), analyzing biological systems becomes more possible.

Fractional order systems are one of the important groups of nonlinear systems. They have been widely used in real-world applications like field-programmable gate array (FPGA) implementation (Tolba et al., 2017) and circuit realization (Tsirimokou et al., 2018). Fractional order systems have different complex properties (Lakshmikantham and Vatsala, 2008; Petráš, 2011). These properties have enabled these systems to be used in modeling of biological phenomena which have shown some complex dynamics in experimental data. For numerical analysis of the fractional order nonlinear system, there are three main approaches, namely the frequency-domain method (Charef, 1992), Adomian decomposition method (ADM) (Adomian, 1990), and Adams-Bashforth-Moulton (ABM) algorithm (Diethelm, 2010). As discussed in Tavazoei and Haeri (2007), the frequency-domain method is not always reliable in detecting chaotic behavior in nonlinear systems. The ABM method is considered to be effective when highly sensitive systems are considered.

To analyze the proposed biological models which are in the group of complex nonlinear dynamical systems, one should consider nonlinear methods like stability of equilibria, Lyapunov exponents, bifurcation diagrams, and the basin of attraction of the system (Hilborn, 2000). As for dynamical diseases, a wide range of diseases are in this nonlinear category. Changes in physiological control parameters cause abnormal dynamics (Bao BC et al., 2018). Thus, to model the dynamical changes in pathophysiological situations, one can change the parameters of the considered model outside the predefined values. The bifurcation diagram and basin of attraction are two methods that can show the dynamics of the model in a wide range of controlling parameters and initial conditions, respectively (Hilborn, 2000). Hence, we use them to evaluate the behavior of the proposed system inside and outside the physiological region.

2 Glucose-insulin regulatory system

A 2D linear differential equation was proposed in Ackerman et al. (1964) to represent the data obtained from the glucose-tolerance test. The proposed mathematical model is as follows:

$$\begin{cases} \dot{x} = a_1 y - a_2 x + c_1, \\ \dot{y} = -a_3 y - a_4 x + c_2 + I, \end{cases} \tag{1}$$

where x and y are the insulin and glucose concentrations respectively and I indicates the rate of increase in blood glucose.

Later, it was discovered that β-cells have an essential role in regulating glucose and insulin concentrations (Bajaj et al., 1987). Note that this was not considered in Ackerman et al. (1964). In Bajaj et al. (1987), a third-order differential equation considering the effect of β-cells was proposed:

$$\begin{cases} \dot{x} = R_1 y - R_2 x + c_1, \\ \dot{y} = \dfrac{1}{2} R_3 N - R_4 x + c_2, \\ \dot{z} = R_5 y (T - z) - R_6 z (T - z) - R_7 z, \end{cases} \tag{2}$$

where z represents the population density of β-cells, N is a constant, and the other parameters are defined in Table 1.

Table 1 Definitions of parameters in Eq. (2)

Parameter	Definition
R_1	Rate of increase in insulin concentration due to blood glucose increase
R_2	Rate of insulin reduction
R_3	Rate of loss of β-cells
R_4	Decrease in rate of glucose in response to insulin generation
R_5	Rate of increase in dividing β-cells due to interaction between blood glucose and β-cells
R_6	Rate of increase in β-cells due to dividing and non-dividing β-cells
R_7	Rate of decrease in β-cells due to its current level
c_1	Constant rate of increase in x
c_2	Constant rate of increase in y
T	Total number of dividing and non-dividing cells

As can be seen, the glucose-insulin relationship is like a predator-prey model, and hence a new model using the Lotka-Volterra model (Elsadany et al., 2012) was developed in Shabestari et al. (2018). In the proposed model, it was assumed that the derivatives of the variables are cubic functions of the state variables. The proposed new model (Shabestari et al., 2018) is as follows:

$$\begin{cases} \dot{x} = -a_1 x + a_2 xy + a_3 y^2 + a_4 y^3 \\ \qquad + a_5 z + a_6 z^2 + a_7 z^3 + a_{20}, \\ \dot{y} = -a_8 xy - a_9 x^2 - a_{10} x^3 + a_{11} y(1-y) \\ \qquad - a_{12} z - a_{13} z^2 - a_{14} z^3 + a_{21}, \\ \dot{z} = a_{15} y + a_{16} y^2 + a_{17} y^3 - a_{18} z - a_{19} yz, \end{cases} \tag{3}$$

where parameters a_1, a_2, a_8, and a_{11} represent the insulin reduction in the absence of glucose, the rate of propagation of insulin in the presence of glucose, the insulin effect on glucose, and the growth of glucose when insulin is absent, respectively. Note that all these parameters are positive. Parameters a_3 and a_4 are the increase in the rate of insulin with increase in glucose; a_5–a_7 are the insulin levels determined by β-cells; a_9 and a_{10} show the insulin effect of glucose level reduction; a_{12}–a_{14} show the effect of insulin secreted by β-cells on the glucose level result; a_{15}–a_{17} show the rate of β-cells with increase in glucose; a_{18} and a_{19} are the decrease in β-cells due to their current level.

Fig. 1 shows the 2D phase portraits of system (3), where the values of parameters are given in Table 2. The initial conditions are taken as (0.53, 1.31, 1.03).

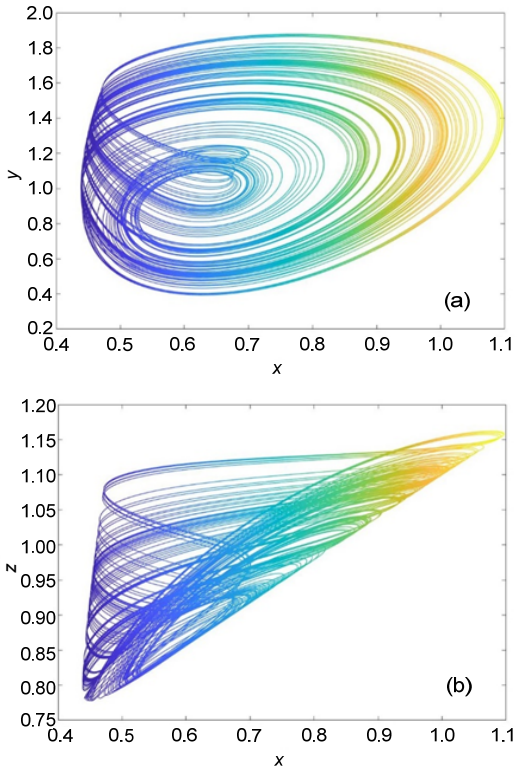

Fig. 1 Two-dimensional phase portraits of system (3) in the *x*-*y* plane (a) and *x*-*z* plane (b)

Table 2 Values of parameters used in system (3)

Parameter	Value	Parameter	Value	Parameter	Value
a_1	2.04	a_8	0.22	a_{15}	0.30
a_2	0.10	a_9	−3.84	a_{16}	−1.35
a_3	1.09	a_{10}	−1.20	a_{17}	0.50
a_4	−1.08	a_{11}	0.30	a_{18}	−0.42
a_5	0.03	a_{12}	1.37	a_{19}	−0.15
a_6	−0.06	a_{13}	−0.30	a_{20}	−0.19
a_7	2.01	a_{14}	0.22	a_{21}	−0.56

3 Fractional order glucose-insulin regulatory system (FOGIRS)

To model biological systems that are memory-dependent, one can use delayed differential and fractional order systems. In this case, fractional order

models give long-time memory and an extra degree of freedom to the system (Rihan et al., 2016). Also, analyzing a system in fractional order is closely related to fractals (Rocco and West, 1999), which are abundant in biological systems. Note that in a more realistic predator-prey model memory effect should be considered; e.g., the predator growth rate at present depends on past quantities of prey, which can be easily accessible if we use fractional order analysis. As this predator-prey system with integer order (Eq. (3)) has been used, we become interested in analyzing the system using fractional derivatives. Apart from this, much recent research has shown that many integer order chaotic systems have complex features like multistability, megastability, and bispectrum when they are investigated as fractional order systems (Rajagopal et al., 2017a, 2017b, 2019). The fractional order form of the glucose-insulin model (Eq. (3)) is derived using the predictor-corrector method (Diethelm, 1997; Diethelm and Ford, 2002). In this section the predict-evaluate-correct-evaluate (PECE) method of ABM studied in Diethelm and Freed (1999) is used. Its convergence and accuracy have been discussed in Diethelm et al. (2004).

Consider the fractional order form of the FOGIRS as

$$\begin{cases} D^{q_x}x = -a_1x + a_2xy + a_3y^2 + a_4y^3 + a_5z \\ \qquad\quad + a_6z^2 + a_7z^3 + a^{20}, \\ D^{q_y}y = -a_8xy - a_9x^2 - a_{10}x^3 + a_{11}y(1-y) \\ \qquad\quad - a_{12}z - a_{13}z^2 - a_{14}z^3 + a_{21}, \\ D^{q_z}z = a_{15}y + a_{16}y^2 + a_{17}y^3 - a_{18}z - a_{19}yz. \end{cases} \tag{4}$$

To derive the general model of the PECE method (Diethelm, 1997; Diethelm and Ford, 2002), consider a fractional order dynamical system with order q as

$$D^q x = f(t,x), \tag{5}$$

where $0\le t\le T$ and $x^k(0)=x_0^k$ for $k\in[0, n-1]$.

Eq. (5) is similar to the Volterra integral equation given by

$$x(t) = \sum_{k=0}^{n-1} x_0^k \frac{t^k}{k!} + \frac{1}{\Gamma(q)}\int_0^t \frac{f(\tau,x)}{(t-\tau)^{1-q}}\mathrm{d}\tau. \tag{6}$$

The discrete form of Eq. (6) can be defined as

$$\begin{aligned} x_h(t_{n+1}) = {} & \sum_{k=0}^{n-1} x_0^{(k)} \frac{t_n^{k+1}}{k!} + \frac{h^q}{\Gamma(q+2)} f\left(t_{n+1}, x_h^p(t_{n+1})\right) \\ & + \frac{h^q}{\Gamma(q+2)} \sum a_{j,n+1} f\left(t_{n+1}, x_h^p(t_{n+1})\right), \end{aligned} \tag{7}$$

where

$$\begin{cases} a_{j,n+1} = \begin{cases} n^{q+1} - (n-q)(n+1)^{q+1}, & j=0, \\ -2(n-j+1)^{q+1}, & 1\le j\le n, \\ 1, & j=n+1, \end{cases} \\ x_h^p(t_{n+1}) = \sum_{k=0}^{n-1} x_0^{(k)} \frac{t_n^{k+1}}{k!} + \frac{h^q}{\Gamma(2)} \sum_{j=0}^{n} b_{j,n+1}\left(t_j x_h(t_j)\right), \\ b_{j,n+1} = \frac{h^q}{q}\left((n-j+1)^q - (n-j)^q\right), \end{cases} \tag{8}$$

$h=T/N$, and $t_n=nh$ with $h\in[0, N]$.

The error estimate is $e=\max|x(t_i)-x_h(t_i)|=0(h^p)$, where $i=0, 1, \ldots, N$ and $p=\min(2, 1+q)$.

Using the above definitions (Eqs. (7) and (8)), the discrete form of FOGIRS can be defined as Eq. (9) with parameters given in Eqs. (10) and (11) (see the next page, $l=1, 2, 3$ and $i=x, y, z$).

Fig. 2 shows the 2D phase portraits of the discretized form of FOGIRS when $q_i=0.995$ and the other parameters are as given in Table 2. Also, the initial conditions are considered as (0.53, 1.31, 1.03).

4 Dynamical analysis of FOGIRS

In this section, we discuss the dynamical properties of FOGIRS, including stability of equilibrium points and Lyapunov exponents.

4.1 Stability of equilibrium points

The dynamical behavior of FOGIRS can be analyzed with the help of eigenvalues. Similar to the discussion in Shabestari et al. (2018), we are interested in the analysis of the positive equilibrium points. The FOGIRS shows two positive equilibrium points, E_1(0.805, 1.815, 1.319) and E_2(0.624, 0.935, 0.877).

Corollary 1 For the FOGIRS to exhibit chaotic dynamics like its integer order form discussed, the necessary condition is

$$\begin{cases} x_{n+1}=x_0+\dfrac{h^{q_x}}{\Gamma(q_x+2)}\Big[-a_1x_{n+1}^p+a_2x_{n+1}^py_{n+1}^p+a_3(y_{n+1}^p)^2+a_4(y_{n+1}^p)^3+a_5z_{n+1}^p+a_6(z_{n+1}^p)^2+a_7(z_{n+1}^p)^3+a_{20}\Big] \\ \quad +\dfrac{h^{q_x}}{\Gamma(q_x+2)}\sum\limits_{j=0}^{n}\Big[\eta_{1,j,n+1}\left(-a_1x_j+a_2x_jy_j+a_3y_j^2+a_4y_j^3+a_5z_j+a_6z_j^2+a_7z_j^3+a_{20}\right)\Big], \\ y_{n+1}=y_0+\dfrac{h^{q_y}}{\Gamma(q_y+2)}\Big[-a_8x_{n+1}^py_{n+1}^p-a_9(x_{n+1}^p)^2-a_{10}(x_{n+1}^p)^3+a_{11}y_{n+1}^p(1-y_{n+1}^p)-a_{12}z_{n+1}^p-a_{13}(z_{n+1}^p)^2-a_{14}(z_{n+1}^p)^3 \\ \quad +a_{21}\Big]+\dfrac{h^{q_y}}{\Gamma(q_y+2)}\sum\limits_{j=0}^{n}\Big\{\eta_{2,j,n+1}\Big[-a_8x_jy_j-a_9x_j^2-a_{10}x_j^3+a_{11}y_j(1-y_j)-a_{12}z_j-a_{13}z_j^2-a_{14}z_j^3+a_{21}\Big]\Big\}, \\ z_{n+1}=z_0+\dfrac{h^{q_z}}{\Gamma(q_z+2)}\Big[a_{15}y_{n+1}^p+a_{16}(y_{n+1}^p)^2+a_{17}(y_{n+1}^p)^3-a_{18}z_{n+1}^p-a_{19}y_{n+1}^pz_{n+1}^p\Big]+\dfrac{h^{q_z}}{\Gamma(q_z+2)}\sum\limits_{j=0}^{n}\Big[\eta_{3,j,n+1}\left(a_{15}y_j \\ \quad +a_{16}y_j^2+a_{17}y_j^3-a_{18}z_j-a_{19}y_jz_j\right)\Big], \end{cases} \tag{9}$$

$$\begin{cases} x_{n+1}^p=x_0+\dfrac{1}{\Gamma(q_x+2)}\sum\limits_{j=0}^{n}\omega_{1,j,n+1}\left(-a_1x_j+a_2x_jy_j+a_3y_j^2+a_4y_j^3+a_5z_j+a_6z_j^2+a_7z_j^3+a_{20}\right), \\ y_{n+1}^p=y_0+\dfrac{1}{\Gamma(q_y+2)}\sum\limits_{j=0}^{n}\Big\{\omega_{2,j,n+1}\Big[-a_8x_jy_j-a_9x_j^2-a_{10}x_j^3+a_{11}y_j(1-y_j)-a_{12}z_j \\ \quad -a_{13}z_j^2-a_{14}z_j^3+a_{21}\Big]\Big\}, \\ z_{n+1}^p=z_0+\dfrac{1}{\Gamma(q_z+2)}\sum\limits_{j=0}^{n}\omega_{3,j,n+1}\left(a_{15}y_j+a_{16}y_j^2+a_{17}y_j^3-a_{18}z_j-a_{19}y_jz_j\right), \end{cases} \tag{10}$$

$$\begin{cases} \eta_{l,j,n+1}=\begin{cases} n^{q_i+1}-(n-q_i)(n+1)^{q_i+1}, & j=0, \\ (n-j+2)^{q_i+1}+(n-j)^{q_i+1}-2(n-j+1)^{q_i+1}, & 1\le j\le n, \\ 1, & j=n+1, \end{cases} \\ \omega_{l,j,n+1}=\dfrac{h^{q_i}}{q_i}\left((n-j+1)^{q_i}-(n-j)^{q_i}\right), \quad 0\le l\le n. \end{cases} \tag{11}$$

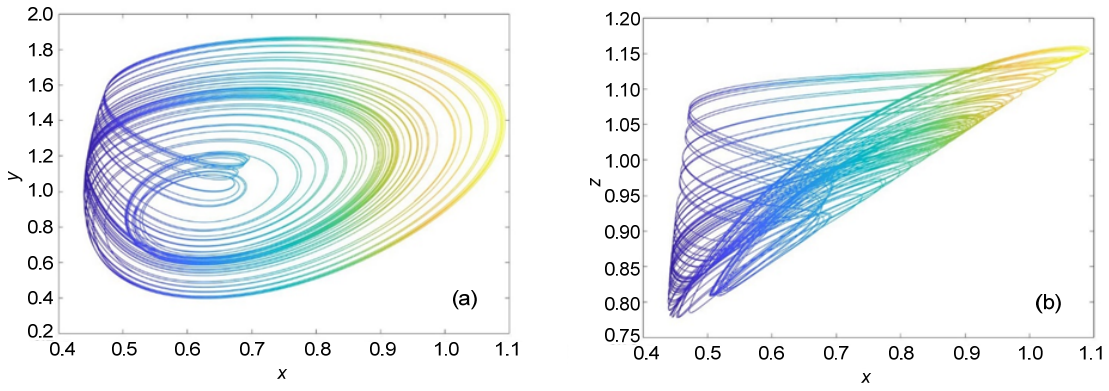

Fig. 2 Two-dimensional phase portraits of the discretized FOGIRS in the *x*-*y* plane (a) and *x*-*z* plane (b)

$$q > \frac{2}{\pi}\arctan\left(\frac{|\mathrm{Im}(\lambda)|}{\mathrm{Re}(\lambda)}\right) \tag{12}$$

for any λ of the equilibrium points.

The eigenvalues of Eq. (3) at equilibrium E_1 are $\lambda_{1,2}$=−1.7564±7.5090i and λ_3=1.3802; to satisfy condition (12), we have q_i>0.86. Similarly, the eigenvalues of Eq. (3) at equilibrium E_2 are $\lambda_{1,2}$=0.5262±2.3472i and λ_3=−2.8372, and we should have q_i>0.85 for i=x, y, z to satisfy condition (12).

Corollary 2 For the chaotic attractor to exist in FOGIRS as in the integer order model (Shabestari et al., 2018), the equilibrium points corresponding to the oscillations should exhibit instability. Hence, the necessary condition for unstable equilibrium existence is

$$\frac{\pi}{2M} - \min_i\{\arg(\lambda_i)\} \geq 0, \tag{13}$$

where λ_i are the roots of $\det\left(\mathrm{diag}\left(\lambda^{Mq_x}, \lambda^{Mq_y}, \lambda^{Mq_z}\right) - \boldsymbol{J}_{E_i}\right) = 0$ for each E_i (i=1, 2).

From Corollaries 1 and 2, we can conclude that FOGIRS exhibits chaotic dynamics when q_i>0.86 for E_1 and q_i>0.85 for E_2, where i=x, y, z.

4.2 Lyapunov exponents

The Lyapunov exponents (LEs) of FOGIRS are derived using the Wolfs algorithm (Wolf et al., 1985) and the fractional order predictor-corrector (Diethelm and Freed, 1999) solver fde12 (Garrappa, 2011) instead of the ordinary differential equation (ODE) solvers (Danca, 2015). The Lyapunov exponents of FOGIRS when the parameters are set to the values in Table 1 and commensurate fractional order q_i>0.85, are numerically found as L_1=0.166, L_2=0, and L_3=−1.98. Since there is a positive Lyapunov exponent, FOGIRS exhibits chaotic oscillations. The Kaplan-Yorke dimension of FOGIRS is also calculated, i.e., D_{KY}=2.09.

5 Numerical analysis of FOGIRS in different glucose-insulin arrhythmias

In this section, we discuss different types of glucose and insulin related disorders, by investigating the respective bifurcation diagrams. Considering the fractional order form of the glucose-insulin model can reveal important features like multistability and co-existing attractors. In this study, we consider the FOGIRS model and derive the bifurcation plots.

5.1 Type-2 diabetes

The type-2 diabetes is a disorder due to the rise in the glucose level in the blood. There may be two reasons for the glucose level rise. The first is when the human body becomes resistant to insulin and the second is when the human body cannot track the glucose level. The parameter a_8 in Eq. (9) represents the effect of secreted insulin on the glucose level. Studying the bifurcation of a_8 is important for understanding the effect of insulin on the glucose level and the resulting chaotic dynamics. We consider the commensurate fractional order of the system when q_i=0.995 and the other parameters are fixed to the values in Table 2. The initial transitions are removed and the local maxima of the state variable x denoting the population density of insulin are plotted against a_8 (varying from 0 to 0.9) (Fig. 3). As can be seen from Fig. 3, the system takes a period doubling route to chaos. The sensitive nature of FOGIRS can be observed from the chaotic dynamics shown by the bifurcation plot. Clinically, the key elements playing the significant role in such sensitive behavior are the shape and volume of the cells. These are related to electrical activities and play a main role in insulin secretion.

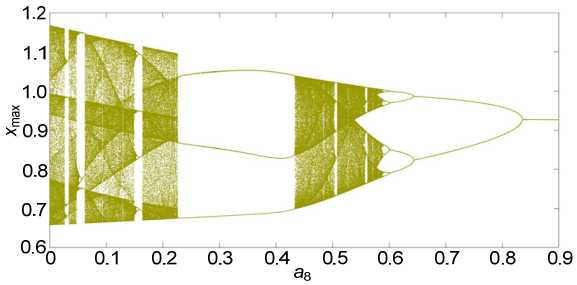

Fig. 3 Bifurcation diagram of FOGIRS when a_8 varies from 0 to 0.9, q_i=0.995, and the other parameters are fixed to the values in Table 2

5.2 Hypoglycemia

Excessive secretion of insulin in blood is known as hypoglycemia. This is directly related to parameter a_1, and the other parameters are fixed to the values in

Table 2 in the FOGIRS model. Depending on the increase or decrease in parameter a_1, FOGIRS behaves chaotically. Parameter a_1 varies from 1.5 to 2.6 and the local maxima of z are plotted. It is interesting to note that the bifurcation plot shown in Fig. 4 exhibits the property of antimonotonicity (referring to period doubling and inverse period doubling occurrence) for $a_1 \in [1.70, 1.74]$. To check the existence of multistability, we consider forward bifurcation where the parameter increases with reinitializing the initial condition to the end value of the previous trajectory and backward bifurcation where the parameter decreases. In Fig. 5a, we show forward bifurcation in blue and backward bifurcation in red. Fig. 5d shows the specified region of Fig. 5a which contains multistability. The corresponding Lyapunov exponents for FOGIRS are shown in Fig. 5b (forward) and Fig. 5c (backward). The coexisting attractors of FOGIRS for q_i=0.995 are given in Fig. 6. Note that such properties do not exist in the integer order form of the model, which was discussed in Shabestari et al. (2018).

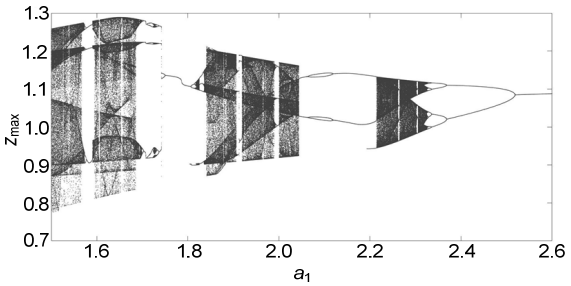

Fig. 4 Bifurcation diagram of FOGIRS when a_1 varies from 1.5 to 2.6 and the other parameters are fixed to the values in Table 2

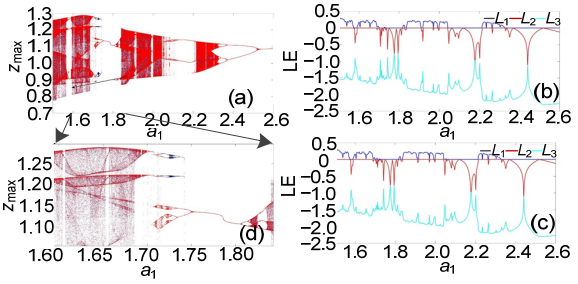

Fig. 5 Bifurcation diagram and Lyapunov exponents of FOGIRS as parameter a_1 changes: (a) forward and backward bifurcation diagrams of FOGIRS; (b) LEs of FOGIRS changing the parameter in forward continuation; (c) LEs of FOGIRS changing the parameter in backward continuation; (d) specified portion with multistability

References to color refer to the online version of this figure

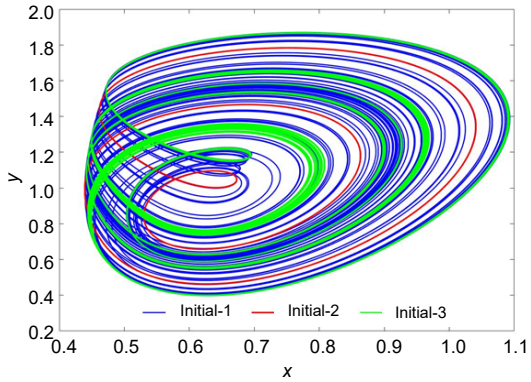

Fig. 6 Coexisting attractors for different initial conditions ((0, 1.5, 1), (0.5, 1, 1), (1.4, −1.5, 1.31)) when commensurate fractional order q_i=0.995 and other parameters are as mentioned in Table 2

References to color refer to the online version of this figure

5.3 Hyperinsulinemia

The permanent over-stimulation of insulin from β-cells of pancreas due to the high glucose level is known as hyperinsulinemia. Parameter a_7 in the FOGIRS model refers to the amplification rate of secretion of insulin by β-cells. The bifurcation of FOGIRS with regard to parameter a_7 is shown in Fig. 7. Increasing a_7 from 1.5 will make FOGIRS enter chaotic dynamics with period doubling. Such undesirable behavior of the system confirms the unstable nature of insulin secretion by β-cells.

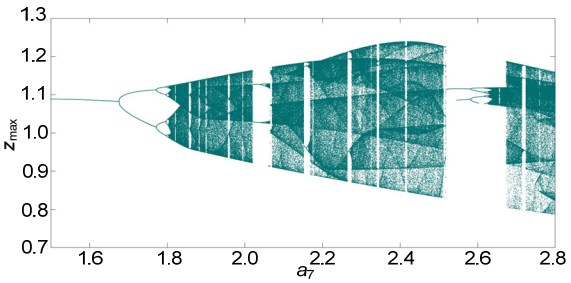

Fig. 7 Bifurcation diagram of FOGIRS with regard to parameter a_7

5.4 Type-1 diabetes

The decrease in population density of β-cells in the pancreas due to autoimmune destruction is termed type-1 diabetes. In the proposed model, parameter a_{15}

corresponds to the rate of increase in the population density of β-cells. If the population density of β-cells decreases, the glucose level cannot be stabilized because of the insufficient secretion of insulin. So, we derive the bifurcation of FOGIRS with regard to a_{15} (Fig. 8). We can again notice the period doubling and period halving bifurcations in Fig. 8, which confirm the property of antimonotonicity.

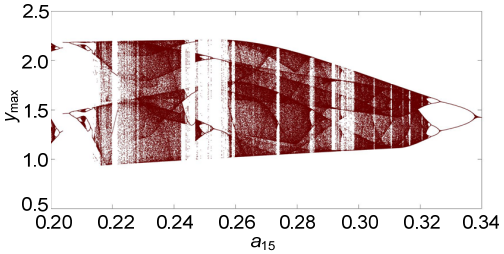

Fig. 8 Bifurcation diagram of FOGIRS with regard to parameter a_{15}

5.5 Bifurcation with fractional order

To show the impact of fractional order on FOGIRS, we consider the commensurate fractional order as the bifurcation parameter, and the local maxima of y are plotted in Fig. 9. Note that the phenomenon of antimonotonicity in the bifurcation plot has not been reported in any earlier fractional order literature. It can also be seen that the system shows more complex behavior in the fractional order range $0.994 \leq q_i \leq 0.997$ for $i \in \{x, y, z\}$. This confirms our claim that fractional order analysis can help us better understand and model more complex behaviors than integer order analysis.

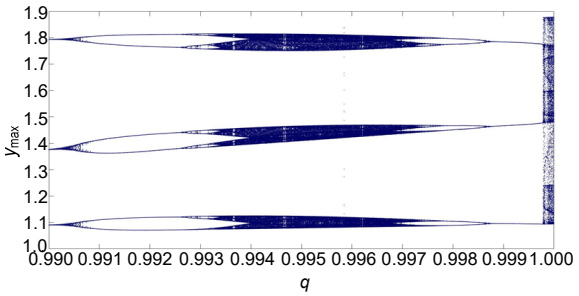

Fig. 9 Bifurcation diagram of FOGIRS for different values of the fractional order of the system

Fig. 10 shows the 2D bifurcation diagram of the FOGIRS system when q_i=0.995. The two parameters considered for the analysis are a_3 which represents the increase in the rate of insulin with increase in glucose and a_8 which represents the insulin effect on glucose.

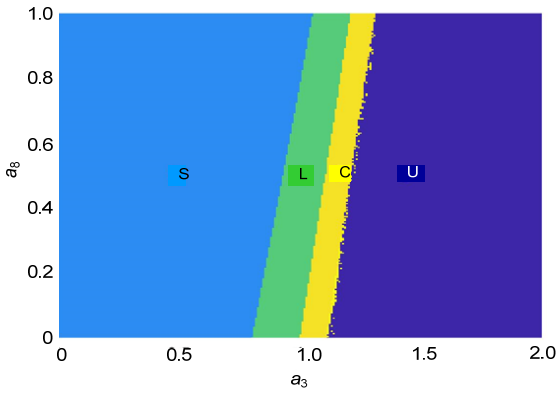

Fig. 10 Two-dimensional bifurcation diagram of FOGIRS for parameters a_3 and a_8

Regions "U," "C," "L," and "S" show the parameter values leading to unbounded response, strange attractor, limit cycle, and stable converging orbit, respectively

5.6 Basin of attraction

A chaotic system whose basin of attraction has an equilibrium point is called a self-excited attractor and one whose basin does not have any equilibrium point is called a hidden attractor (Leonov et al., 2011, 2012; Dudkowski et al., 2016). There have been studies showing that such hidden oscillations are seen in many real-life physical systems (Leonov et al., 2015a, 2015b) and considering the control of the complex attractor in such systems (Sharma et al., 2015a, 2015b). We derive the basin of attraction of FOGIRS for two different cases. The first is when a_1=2.04, y=1.31, and q_i=0.995. Here the system shows a self-excited attractor. The cross-section of basin of attraction is shown in Fig. 11a with the two fixed points shown in red dots. The blue color shows the initial conditions that lead to unbounded oscillations, and the yellow color shows the initial conditions that lead to a strange attractor. Fig. 11b shows the second case when a_1=2.04, z=1.03, and q_i=0.996, for which FOGIRS has no defined equilibrium points and hence the attractor is hidden.

6 Conclusions

The interaction between glucose-insulin and β-cells plays an important role in glucose-insulin

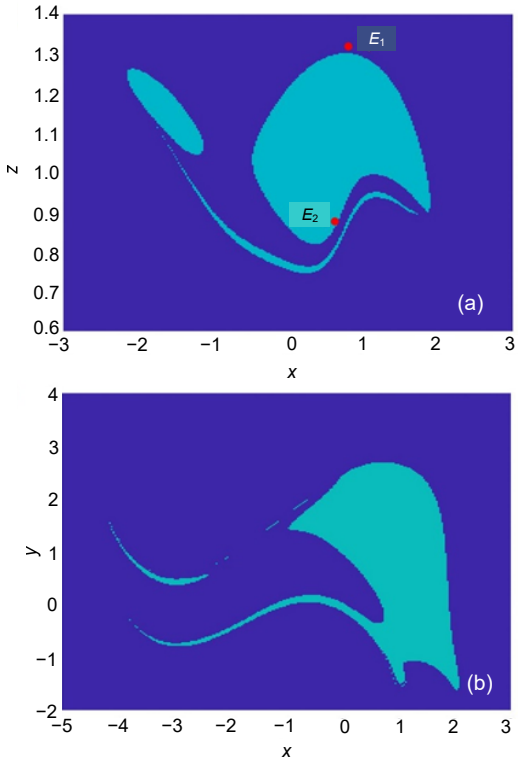

Fig. 11 Cross-section of the basin of attraction of FO-GIRS for the self-excited case (equilibrium points existing in the basin of attraction of the strange attractor) when y=1.31 (a) and the hidden oscillation case when z=1.03 (b)

References to color refer to the online version of this figure

regulation. Recently, a new glucose-insulin regulation model was derived using a predator-prey system. In this study a fractional order model of that new system has been derived. The PECE method of discretization has been adopted to numerically analyze the proposed fractional order model. Various dynamical properties have been derived and presented. Also, the condition for the existence of chaotic oscillations in the fractional order model has been derived and presented. The proposed fractional order model exhibited the properties of coexisting attractors and antimonotonicity which have not been reported in the literature. For future research, controlling this biological fractional order system with a fractional order proportional-integral-derivative (PID) controller (Zhao et al., 2005; Caponetto et al., 2010) and sliding mode control (Chen et al., 2012; Yin et al., 2012) can be considered.

Compliance with ethics guidelines

Karthikeyan RAJAGOPAL, Atiyeh BAYANI, Sajad JAFARI, Anitha KARTHIKEYAN, and Iqtadar HUSSAIN declare that they have no conflict of interest.

References

Ackerman E, Rosevear JW, McGuckin WF, 1964. A mathematical model of the glucose-tolerance test. *Phys Med Biol*, 9(2):203-213. https://doi.org/10.1088/0031-9155/9/2/307

Adomian G, 1990. A review of the decomposition method and some recent results for nonlinear equations. *Math Comput Model*, 13(7):17-43. https://doi.org/10.1016/0895-7177(90)90125-7

Aram Z, Jafari S, Ma J, et al., 2017. Using chaotic artificial neural networks to model memory in the brain. *Commun Nonl Sci Numer Simul*, 44:449-459. https://doi.org/10.1016/j.cnsns.2016.08.025

Baghdadi G, Jafari S, Sprott JS, et al., 2015. A chaotic model of sustaining attention problem in attention deficit disorder. *Commun Nonl Sci Numer Simul*, 20(1):174-185. https://doi.org/10.1016/j.cnsns.2014.05.015

Bajaj JS, Rao GS, Rao JS, et al., 1987. A mathematical model for insulin kinetics and its application to protein-deficient (malnutrition-related) diabetes mellitus (PDDM). *J Theor Biol*, 126(4):491-503. https://doi.org/10.1016/S0022-5193(87)80154-6

Bao BC, Wu PY, Bao H, et al., 2018. Numerical and experimental confirmations of quasi-periodic behavior and chaotic bursting in third-order autonomous memristive oscillator. *Chaos Sol Fract*, 106:161-170. https://doi.org/10.1016/j.chaos.2017.11.025

Bao H, Wang N, Bao BC, et al., 2018. Initial condition-dependent dynamics and transient period in memristor-based hypogenetic jerk system with four line equilibria. *Commun Nonl Sci Numer Simul*, 57:264-275. https://doi.org/10.1016/j.cnsns.2017.10.001

Buscarino A, Fortuna L, Frasca M, et al., 2018. Synchronization of chaotic systems with activity-driven time-varying interactions. *J Compl Netw*, 6(2):173-186. https://doi.org/10.1093/comnet/cnx027

Caponetto R, Dongola G, Fortuna L, et al., 2010. New results on the synthesis of FO-PID controllers. *Commun Nonl Sci Numer Simul*, 15(4):997-1007. https://doi.org/10.1016/j.cnsns.2009.05.040

Charef A, Sun HH, Tsao YY, et al., 1992. Fractal system as represented by singularity function. *IEEE Trans Autom Contr*, 37(9):1465-1470. https://doi.org/10.1109/9.159595

Chen DY, Liu YX, Ma XY, et al., 2012. Control of a class of fractional-order chaotic systems via sliding mode. *Nonl Dynam*, 67(1):893-901. https://doi.org/10.1007/s11071-011-0002-x

Chuedoung M, Sarika W, Lenbury Y, 2009. Dynamical analysis

of a nonlinear model for glucose-insulin system incorporating delays and β-cells compartment. *Nonl Anal Theory Methods Appl*, 71(12):e1048-e1058. https://doi.org/10.1016/j.na.2009.01.129

Danca MF, 2015. Lyapunov exponents of a class of piecewise continuous systems of fractional order. *Nonl Dynam*, 81(1-2):227-237. https://doi.org/10.1007/s11071-015-1984-6

Diethelm K, 1997. An algorithm for the numerical solution of differential equations of fractional order. *Electron Trans Numer Anal*, 5:1-6.

Diethelm K, 2010. The Analysis of Fractional Differential Equations: an Application-Oriented Exposition Using Differential Operators of Caputo Type. Springer, Berlin, Germany. https://doi.org/10.1007/978-3-642-14574-2

Diethelm K, Ford NJ, 2002. Analysis of fractional differential equations. *J Math Anal Appl*, 265(2):229-248. https://doi.org/10.1006/jmaa.2000.7194

Diethelm K, Freed AD, 1999. The FracPECE subroutine for the numerical solution of differential equations of fractional order. Proc Forschung und Wissenschaftliches Rechnen, p.57-71.

Diethelm K, Ford NJ, Freed AD, 2004. Detailed error analysis for a fractional Adams method. *Numer Algor*, 36(1):31-52. https://doi.org/10.1023/B:NUMA.0000027736.85078.be

Dudkowski D, Jafari S, Kapitaniak T, et al., 2016. Hidden attractors in dynamical systems. *Phys Rep*, 637:1-50. https://doi.org/10.1016/j.physrep.2016.05.002

Elsadany AEA, El-Metwally HA, Elabbasy EM, et al., 2012. Chaos and bifurcation of a nonlinear discrete prey-predator system. *Comput Ecol Softw,* 2(3):169-180.

Garrappa R, 2011. Predictor-corrector PECE Method for Fractional Differential Equations. MATLAB Central.

Ginoux JM, Ruskeepää H, Perc M, et al., 2018. Is type 1 diabetes a chaotic phenomenon? *Chaos Sol Fract*, 111:198-205. https://doi.org/10.1016/j.chaos.2018.03.033

Ginoux JM, Naeck R, Ruhomally YB, et al., 2019. Chaos in a predator–prey-based mathematical model for illicit drug consumption. *Appl Math Comput*, 347:502-513. https://doi.org/10.1016/j.amc.2018.10.089

Hadaeghi F, Golpayegani MRH, Jafari S, et al., 2016. Toward a complex system understanding of bipolar disorder: a chaotic model of abnormal circadian activity rhythms in euthymic bipolar disorder. *Aust New Zealand J Psych*, 50(8):783-792. https://doi.org/10.1177/0004867416642022

Hansen K, 1923. Oscillations in the blood sugar in fasting normal persons. *J Int Med*, 57(S4):27-32. https://doi.org/10.1111/j.0954-6820.1923.tb16365.x

Hilborn RC, 2000. Chaos and Nonlinear Dynamics: an Introduction for Scientists and Engineers (2nd Ed.). Oxford University Press, Oxford, USA.

Holt TA, 2003. Nonlinear dynamics and diabetes control. *Endocrinologist*, 13(6):452-456. https://doi.org/10.1097/01.ten.0000089917.44590.5d

Korn H, Faure P, 2003. Is there chaos in the brain? II. Experimental evidence and related models. *Comptes Rendus Biol*, 326(9):787-840. https://doi.org/10.1016/j.crvi.2003.09.011

Kroll MH, 1999. Biological variation of glucose and insulin includes a deterministic chaotic component. *Biosystems*, 50(3):189-201. https://doi.org/10.1016/S0303-2647(99)00007-6

Kumar PRAV, Sreedevi V, 2017. A review on influence of antidiabetic medications on quality of life. *Eur J Pharm Med Res*, 4(5):276-288.

Lakshmikantham V, Vatsala AS, 2008. Basic theory of fractional differential equations. *Nonl Anal Theory Methods Appl*, 69(8):2677-2682. https://doi.org/10.1016/j.na.2007.08.042

Lang DA, Matthews DR, Peto J, et al., 1979. Cyclic oscillations of basal plasma glucose and insulin concentrations in human beings. *N Engl J Med*, 301(19):1023-1027. https://doi.org/10.1056/NEJM197911083011903

Leonov GA, Kuznetsov NV, Vagaitsev VI, 2011. Localization of hidden Chua's attractors. *Phys Lett A*, 375(23):2230-2233. https://doi.org/10.1016/j.physleta.2011.04.037

Leonov GA, Kuznetsov NV, Vagaitsev VI, 2012. Hidden attractor in smooth Chua systems. *Phys D*, 241(18):1482-1486. https://doi.org/10.1016/j.physd.2012.05.016

Leonov GA, Kuznetsov NV, Mokaev TN, 2015a. Hidden attractor and homoclinic orbit in Lorenz-like system describing convective fluid motion in rotating cavity. *Commun Nonl Sci Numer Simul*, 28(1-3):166-174. https://doi.org/10.1016/j.cnsns.2015.04.007

Leonov GA, Kuznetsov NV, Mokaev TN, 2015b. Homoclinic orbits, and self-excited and hidden attractors in a Lorenz-like system describing convective fluid motion. *Eur Phys J Spec Top*, 224(8):1421-1458. https://doi.org/10.1140/epjst/e2015-02470-3

Liszka-Hackzell JJ, 1999. Prediction of blood glucose levels in diabetic patients using a hybrid AI technique. *Comput Biomed Res*, 32(2):132-144. https://doi.org/10.1006/cbmr.1998.1506

Molnar GD, Taylor WF, Langworthy AL, 1972. Plasma immunoreactive insulin patterns in insulin-treated diabetics. Studies during continuous blood glucose monitoring. *Mayo Clin Proc*, 47(10):709-719.

Petráš I, 2011. Fractional-Order Nonlinear Systems: Modeling, Analysis and Simulation. Springer, Berlin, Germany. https://doi.org/10.1007/978-3-642-18101-6

Pfeiffer EF, Meyerhoff C, Bischof F, et al., 1993. On line continuous monitoring of subcutaneous tissue glucose is feasible by combining portable glucosensor with microdialysis. *Horm Metab Res*, 25(2):121-124. https://doi.org/10.1055/s-2007-1002057

Pham VT, Frasca M, Caponetto R, et al., 2012. Control and synchronization of fractional-order differential equations of phase-locked loop. *Chaot Model Simul*, 4:623-631.

Preissl H, Lutzenberger W, Pulvermüller F, 1996. Is there chaos in the brain? *Behav Brain Sci*, 19(2):307-308. https://doi.org/10.1017/S0140525X00042825

Rajagopal K, Akgul A, Jafari S, et al., 2017a. Chaotic chameleon: dynamic analyses, circuit implementation, FPGA design and fractional-order form with basic analyses. *Chaos Sol Fract*, 103:476-487. https://doi.org/10.1016/j.chaos.2017.07.007

Rajagopal K, Karthikeyan A, Srinivasan AK, 2017b. FPGA implementation of novel fractional-order chaotic systems with two equilibriums and no equilibrium and its adaptive sliding mode synchronization. *Nonl Dynam*, 87(4): 2281-2304. https://doi.org/10.1007/s11071-016-3189-z

Rajagopal K, Karthikeyan A, Duraisamy P, et al., 2019. Bifurcation, chaos and its control in a fractional order power system model with uncertainties. *Asian J Contr*, 21(1): 184-193. https://doi.org/10.1002/asjc.1826

Rihan FA, Hashish A, Al-Maskari F, et al., 2016. Dynamics of tumor-immune system with fractional-order. *J Tumor Res*, 2(1):1000109J.

Rocco A, West BJ, 1999. Fractional calculus and the evolution of fractal phenomena. *Phys A*, 265(3-4):535-546. https://doi.org/10.1016/S0378-4371(98)00550-0

Schiff SJ, Jerger K, Duong DH, et al., 1994. Controlling chaos in the brain. *Nature*, 370(6491):615-620. https://doi.org/10.1038/370615a0

Shabestari PS, Panahi S, Hatef B, et al., 2018. A new chaotic model for glucose-insulin regulatory system. *Chaos Sol Fract*, 112:44-51. https://doi.org/10.1016/j.chaos.2018.04.029

Sharma PR, Shrimali MD, Prasad A, et al., 2015a. Control of multistability in hidden attractors. *Eur Phys J Spec Top*, 224(8):1485-1491. https://doi.org/10.1140/epjst/e2015-02474-y

Sharma PR, Shrimali MD, Prasad A, et al., 2015b. Controlling dynamics of hidden attractors. *Int J Bifurc Chaos*, 25(4): 1550061. https://doi.org/10.1142/S0218127415500613

Tavazoei MS, Haeri M, 2007. Unreliability of frequency-domain approximation in recognising chaos in fractional-order systems. *IET Signal Process*, 1(4):171-181. https://doi.org/10.1049/iet-spr:20070053

Tolba MF, AbdelAty AM, Soliman NS, et al., 2017. FPGA implementation of two fractional order chaotic systems. *AEU-Int J Electron Commun*, 78:162-172. https://doi.org/10.1016/j.aeue.2017.04.028

Tsirimokou G, Psychalinos C, Elwakil AS, et al., 2018. Electronically tunable fully integrated fractional-order resonator. *IEEE Trans Circ Syst II*, 65(2):166-170. https://doi.org/10.1109/TCSII.2017.2684710

Wolf A, Swift JB, Swinney HL, et al., 1985. Determining Lyapunov exponents from a time series. *Phys D*, 16(3): 285-317. https://doi.org/10.1016/0167-2789(85)90011-9

Yin C, Zhong SM, Chen WF, 2012. Design of sliding mode controller for a class of fractional-order chaotic systems. *Commun Nonl Sci Numer Simul*, 17(1):356-366. https://doi.org/10.1016/j.cnsns.2011.04.024

Zhao CN, Xue DY, Chen YQ, 2005. A fractional order PID tuning algorithm for a class of fractional order plants. Proc IEEE Int Conf on Mechatronics and Automation, p.216-221. https://doi.org/10.1109/ICMA.2005.1626550